sciendo

Green Sciences, 27, 4, 20—33, 10.2478/pjct-2025-0018

Electrocoagulation and Coupled Processes for Urea Wastewater Removal: Parametric study and gradient boosting optimization.

Wafa Atba[1], Mouna Cherifi[1], Sabir Hazourli[1], Amel Boulmaiz[2], François Lapicque[3], Azzeddine Grid[4], Debra F. Laefer[5]

[1]Laboratory of Water Treatment and Valorization of Industrial Wastes, Badji Mokhtar- Annaba University. 12. P.O. Box, 23000 Annaba. Algeria
[2]Laboratory of Applied Biochemistry and Microbiology, Badji Mokhtar- Annaba University. 12. P.O. Box, 23000 Annaba. Algeria
[3]University of Lorraine, CNRS, LRGP, 54000, Nancy, France
[4]Research Center in Technological Industries (CRTI), P.O. Box 64, Cheraga 16014 Algiers, Algeria
[5]Department of Civil and Urban Engineering, Tandon School of Engineering, New York University, 6 Metrotech, Brooklyn, New York, 11201, United States
[*]*Corresponding author:* e-mail: wafa.atba@univ-annaba.dz

This study investigates urea removal from wastewater using zinc-based electrocoagulation method, supported by Gradient Boosting Regressor modeling. The highest urea removal of 42% was obtained for 1.2 g/L initial urea concentration, 22 mA/cm^2 current density, and a pH solution of 10, while natural pH (≈7.50) gave 30%. By applying the optimum conditions 27% of urea was removed from real hospital effluent. Application of GBR model leveraging Artificial Intelligence (AI) demonstrated a high predictive accuracy (R^2 = 0.9825, RMSE = 0.01666) with experimental results. Treatment combination processes were investigated: Chemical Coagulation–Electrocoagulation achieved 35% efficiency, while two EC cycles yielded 45%. Electrocoagulated sludge characterization by scanning electron microscope/ energy-dispersive X-ray spectroscopy, Fourier-transform infrared spectroscopy, X-ray diffraction analysis revealed surface irregularities as well as the presence of zinc, carbon, nitrogen, and sodium. These findings confirm the treatment's effectiveness in removing urea and support the safe valorization and reuse of the sludge. EC proves effective and cost-efficient for industrial-scale implementation.

Keywords: Urea removal; Electrocoagulation; Gradient Boosting Regressor; Sludge characterization; Hospital effluent.

Received: 20 June 2025; Accepted: 19 September 2025; Available online: 14.01.2026.

INTRODUCTION

In modern chemistry, urea is recognized as a fundamental molecule notable for being the first organic compound synthesized entirely from inorganic substances[1, 2]. Urea, a by-product of protein metabolism in mammals, is a common pollutant caused by organic urea plant fertilizers used, domestic wastewater, erosion, and runoff from agricultural soils[3–5].

Although nontoxic, urea at basic pH can naturally hydrolyze into ammonium and then to ammonia. The ammonia tends to volatilize, causing pollution and a potential danger, particularly in an aqueous environment[4, 5]. In wastewater and with increasingly stringent environmental regulations, the maximum allowable concentration of urea in effluent is 10 mg/L[6]. So, it is essential to reduce urea concentrations at wastewater treatment plants[2, 7].

Several methods have been used for the removal of urea, including physico-chemical methods such as adsorption[8], hydrolysis[9], catalytic decomposition[10] or electrochemical techniques[11]. Biological treatments were also tested[12]. Among those, electrocoagulation (EC) is environmentally friendly, simple, versatile, reliable, and cost-effective. More generally, EC has an exceptional ability to efficiently remove a range of pollutants from water, while generating minimal sludge[13, 14].

Traditional chemical coagulation disrupts the stability of particles or dissolved substances in water by adding di- or trivalent salts, which hydrolyze into coagulants. These destabilize pollutants that are suspended or dissolved in the water. In contrast, EC generates coagulant species in situ by passing an electric current through a sacrificial anode. Simultaneously, the reduction reaction at the cathode generates hydrogen gas[5, 15]. This method, which combines the benefits of coagulation, flotation, and electrochemistry, has shown promise for wastewater treatment[4, 13, 16].

During EC, the chemical reactions occurring with the (Zn) electrodes are as follows in equations (1–3)[7, 17]:

At the anode:

$$Zn(s) \rightarrow Zn^{2+} + 2e^{-} \quad E_0 = -0.800 \text{ V/NHE} \qquad (1)$$

for coagulation

$$2H_2O \rightarrow 4H+ + O_2 + 4\acute{e} \quad E_0 = -1.23 \text{ V/NHE} \qquad (2)$$

At the cathode:

$$H_2O + 2e^{-} \rightarrow H_2(g) + 2OH^{-} \quad E_0 = -0.828 \text{ V/NHE} \qquad (3)$$

for flotation

Under adequate pH conditions, the resulting Zn^{2+} ions are immediately hydrolyzed to produce corresponding polyhydroxides or hydroxides, thereby effectively destabilizing pollutants, according to equation (4):

$$Zn^{2+} + 2H_2O \rightarrow Zn(OH)_2 + 2H^{+} \qquad (4)$$

The removal mechanism may be through charge neutralization, sweep coagulation, or adsorption. Destabilized pollutants can then be separated from the treated solution either by flotation or settling[18]. Notably, most EC research has used aluminum or iron electrodes as sacrificial anodes. However, recent studies have shown effectiveness using Zinc anodes for the removal of arsenite[19], phenolic compounds[20] and selenium[21], as well

as lead (achieving up to 99.9% removal within 10 minutes)[22]. Among the studies on electrocoagulation (EC) using various electrode materials for urea removal[4, 5, 23], only one employed zinc electrodes[7]. That laboratory work demonstrated promising results using a synthetic aqueous solution.

Optimizing wastewater treatment procedures has to date been time-consuming and resource-intensive, as the process has involved varying only a single parameter at a time despite that the processes involve a wide range of material, concentration, pH-level, temperature, and duration choices. Furthermore, single variable substitutions stymie the ability to understand the interaction effects of all the factors affecting the process[24]. While phenomenological and empirical modeling techniques are necessary in water/wastewater treatment studies[25], there is the potential to improve the optimization process through Artificial Intelligence-based tools such as Adaptive Neuro-Fuzzy Inference System[26, 27], Artificial Neural Network[28] and The Gradient Boosting Regressor[29, 30], are other tools for modeling nonlinear systems[31].

The Gradient Boosting Regressor (GBR) is a non-parametric, machine learning technique used for regression and classification. GBR builds an additive model by sequentially fitting weak models, such as decision trees, to minimize a loss function. This method is particularly useful when theoretical models are not available or when the relationships between input variables are not well understood. Unlike building a single predictive model, GBR creates a set of weak models to achieve a more robust prediction. Formulated using gradient descent, GBR links to a statistical framework, thus justifying model hyperparameters for large, complex data set[29, 32].

Unlike previous studies, which focused on aluminum or iron electrodes, this study presents an in-depth investigation into urea removal by electrocoagulation (EC) using zinc electrodes, combined with predictive modeling with GBR. Specifically, this research examines the effectiveness of zinc electrodes under various operational conditions, including current density, electrolysis time, pH, temperature, conductivity, and initial urea concentration. This is followed by a cost evaluation.

The study also includes an assessment of specific configurations, such as EC combined with chemical coagulation and sequential EC treatment cycles. In this study, electrocoagulation with zinc electrodes was applied to a real effluent—dialysate discharged from hemodialysis clinical services. This step assesses the feasibility of the process under real-world conditions, taking into account the complexity of biological matrices and the competition among dissolved species. Finally, the physico-chemical characterization of the generated electrocoagulation sludge via SEM, EDS, FTIR, and XRD provides further insight into urea capture mechanisms and highlights the potential of its valorization. Finally, an economic analysis was performed for each operational strategy (Fig. 1).

MATERIALS AND METHODS

Synthetic urea effluent

This study sourced urea and sodium chloride of 99% purity from Sigma-Aldrich. All the chemicals were of analytical grade, and ultrapure water was used to prepare all solutions. The zinc electrodes (99.99% purity) were sourced from Science Lab.

Synthetic urea effluent was prepared by dissolving urea and NaCl (purity 99%) in the ultrapure water at a rate of 1.2 g/L of urea and 1.5 g/L of sodium chloride.

Urea Processing Methods

For the EC setup, two zinc plate electrodes (7.5 × 3 × 0.2 cm; active surface area: 22.5 cm^2) were used as anode and cathode. They were placed vertically in a 500 mL beaker containing a synthetic urea solution (1.2 g/L urea and 1.5 g/L NaCl) (Fig. 2). Electrodes were connected to a direct current DC power supply (Metrix AX 502, 30 V, 2.5 A) with an inter-electrode distance of 1.0 cm. The solution was gently stirred at 100 rpm to ensure uniform mixing and prevent foam formation

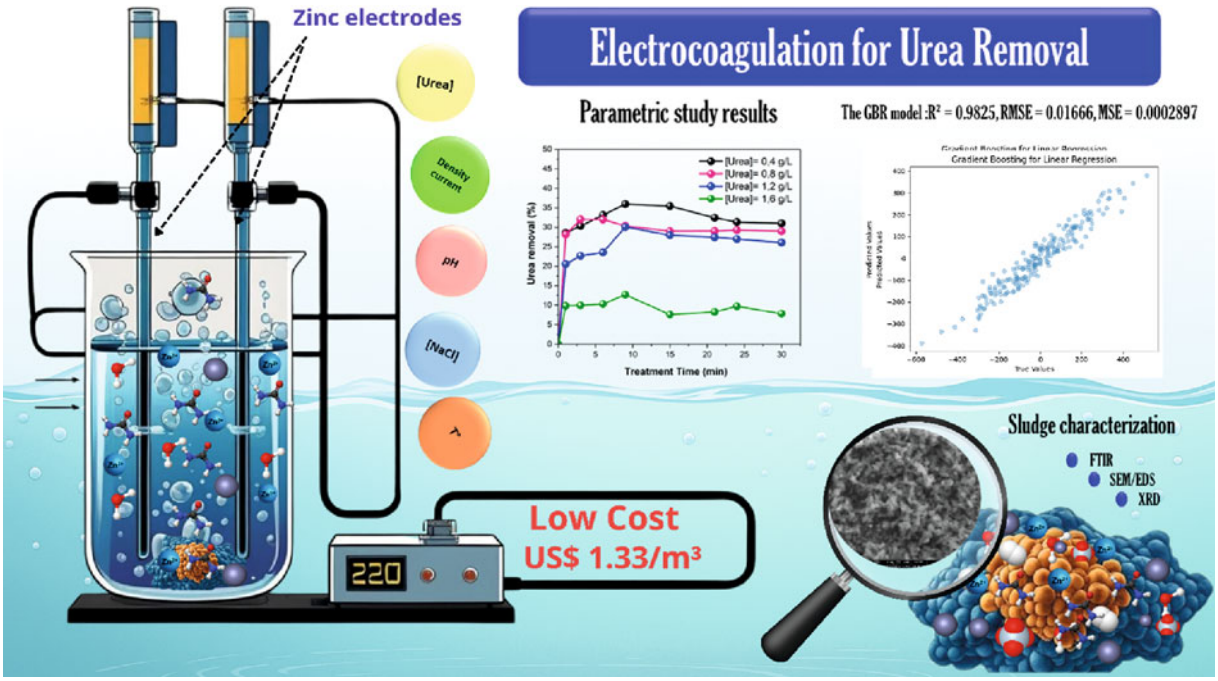

Figure 1. Graphical Abstract

during gas evolution. Experiments were conducted at an ambient temperature (20 ± 2°C). The natural pH of the solution (~7.60) was adjusted to pH 4 or 10 using 0.1 M HCl or NaOH when required. Aliquots (5 mL) were sampled at predetermined intervals, allowed to settle, and filtered through 0.45 µm membranes to determine residual urea in the solution. After each run, the electrodes were rinsed and cleaned with a 15% HCl solution to remove accumulated deposits.

To enhance urea removal, EC operational parameters were modified and followed by the other EC cycles. At the end of each cycle, the treated solution was filtered, and the resulting filtrate was reused as the influent for the subsequent cycle. This process was repeated until four consecutive EC cycles were completed (EC–EC–EC–EC).

In this study, the EC combination, coagulation/flocculation tests were firstly performed using a jar test flocculator (Velp Scientifica C6F). A volume of 500 mL of a urea solution of 1.2 g/L was treated with varying concentrations of zinc sulfate (2–8 g/L) as a commercial coagulant. A fixed amount of polyelectrolyte SP6 (1 mg/L) was added to enhance the floc formation. The protocol included 3 minutes of rapid mixing for homogenization of the solution, followed by 15 minutes of slow stirring to facilitate floc growth, and 30 minutes of settling to clarify the effluent. After that, combined treatment configurations between EC and CC in the optimum operating conditions were implemented: EC followed by chemical coagulation (EC–CC), and chemical coagulation followed by EC (CC–EC).

Figure 2. View of the electrocoagulation setup

Analysis and calculation

Urea removal yield (R)

The concentration of urea was determined using a high-performance liquid chromatography (HPLC) instrument (Shimadzu LC-20 AT) equipped with a C18 column (5 µm, 250 × 4.6 mm). The column operated at a temperature of 40 °C. Samples of 10 μL were injected into the HPLC column. The mobile phase was composed of 25% acetonitrile and 75% ultrapure water, by volume. The flow rate of the mobile phase was set at 1 mL/min. Urea was detected at a wavelength of 198 nm.

The percentage removal efficiency of EC process was computed as a function of operating time by Equation (5)

$$R = \frac{C_0 - C_f}{C_0} * 100 \quad (5)$$

C_0 : initial urea concentration (g/L)
C_f : final urea concentration (g/L)
R: yield removal of urea (%)

The amount of zinc dissolved after 30 min tests was estimated by weighing the two electrodes with 0.1 mg accuracy before and after the tests.

Zn Faraday

Faraday's law is often used to calculate the theoretical amount of released Zn from anode, which can be expressed as Eq (6):

$$m = \frac{ItM}{zF} \quad (6)$$

where m is the released coagulants from the anode (g), M is the atomic weight of the electrodes (M = 65.4 g/mol for Zn), z is the number of electrons transferred in the anodic dissolution, F is the Faraday constant (96486 $C \cdot mol^{-1}$), and t is the electrolysis time in seconds.

Energy consumption

Energy consumption was estimated using Equation (7):

$$EC = (U.I.t)/(3600.V) \quad (7)$$

where EC is energy consumption (kWh/m^3), U is the voltage (in volts), V denotes the solution volume (L), I is the applied current (A), and t is the operating time (s).

Operating cost

Operating costs are critical, as they indicate viability. Herein, they were evaluated using equation 8, which includes energy and consumable costs.

$$OC = \mathrm{EC} + Electrode_{consumption} + Chemical_{consumption} \quad (8)$$
$$(X_1.Enery_{consumption}) + (X_2.Electrode_{consumption}) +$$
$$+ (X_3.Chemical_{consumption})$$

Where OC is total operating cost per m^3 of treated water (US$/m^3), X_1 represents the unit price of the Zn electrode (3.1 USD/kg), X_2 represents the unit price of electricity (on the Algerian market in January 2025, the cost of electrical energy was US$ 0,041 /kWh for the first 125 kWh and US$ 0,036 /kWh above 125 kWh), and X_3 represents the unit price of zinc sulfate (US$ 2.1/Kg).

Machine Learning analysis

After the experimental program was complete, GBR was applied to the full experimental dataset using Python in a Jupyter Notebook of Anaconda Navigator 2.5.0. This enabled exploration and modeling of the complex relationships between process parameters, with rigorous performance evaluation using statistical indicators (RMSE, MSE, R^2). The regression model was aimed at predicting the current density (target, i.e. output variable) after several fixed values of time depending on the input variables, such as temperature, initial pH, initial concentration, and experimental removal yield. Each successive model version corrects and minimizes the errors of the previous versions by adjusting the residuals of the predictions and improving the model's accuracy[30, 33].

To assess the quality of predictions, the model's performance was evaluated using key statistical indicators: the coefficient of determination (R^2), mean squared

error (MSE), and root mean squared error (RMSE). These indices provide a comprehensive assessment of the model's predictive accuracy. Optimal model performance is indicated by an R^2 value (coefficient of determination) approaching 1, and MSE and RMSE values approaching 0. The mathematical definitions of these statistical indices are provided in Table 1[31], where: y_i = experimental response; y^*_i = predicted response; and $\bar{y}$ = mean value of actual responses.

Table 1: Mathematical representations of the statistical indices.

In addition, to thoroughly evaluate the GBR model's robustness and performance, several further metrics were calculated and analyzed:

1 – Cook distance, which reveals peaks and outliers exceeding the indicative threshold of 4/n, where n is the total number of observations in the sample[34].

2 – The leverage and the impact of outliers when working with multiple regression analysis or confidence intervals for the mean[35].

RESULTS AND DISCUSSION

Effect of electrocoagulation operating parameters

Effect of initial concentration and treatment time

The urea removal rate is known to depend on various parameters, with the electrocoagulation treatment time playing a major role in pollutant removal efficiency[36]. Runs were monitored at different urea concentrations (0.4 g/L – 1.6 g/L), a constant current density of 22 mA/cm^2, and an initial pH of 7.60 for a process of 30 min, while maintaining a 1 cm internal distance between the electrodes. As shown in Figure 3, when the treatment period increased, the urea removal efficiencies were enhanced because of larger Zn(II) and hydroxide ion concentrations[37]. The maximum urea elimination occurred over the first 9 minutes at efficiencies from 13% – 36% with the lower removal percentages aligning with the higher initial urea concentrations (Fig. 3), additional electrolysis time consumed more energy but did not achieve higher elimination levels. After 9 min, there was a slight decrease in removal efficiency, which may be attributable to the formation of dense flocs that would hinder the adsorption of pollutants[36, 38]. The number of hydroxide flocs formed was insufficient to adsorb more urea at a higher initial concentration.

The urea removal rate was clearly hampered by higher initial urea concentrations. Specifically, the removal rate evolution was faster with lower concentrations, and the highest urea removal (36%) was achieved at 0.4 g/L initial urea concentration. However, only 16% was removed at the highest initial concentration of 1.6 g/L. Notably, according to Faraday's law, the amount of dissolution of zinc electrodes should not be affected by the initial pollutant concentration. The production rate of hydroxyl radical and the quantity of $Zn(OH)_2$ flocs formed can be assumed almost constant for the same current density and electrolysis time. However, as reported in previous works[39], increasing pollutant concentration enhances concentration polarization via adsorption on the anode and cathode, thus resulting in to decrease in the Zn dissolution rate at the anode and the hydrogen gas evolution at the cathode[39]. At industrial scale, one must increase the surface of electrodes used, while keeping a constant current density to achieve the same removal efficiency as in this study.

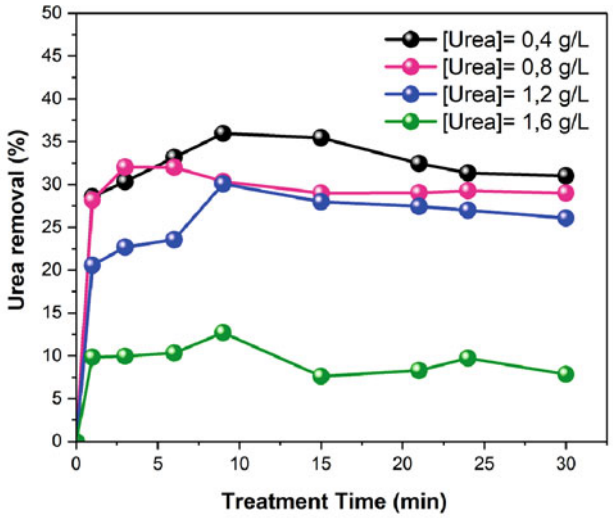

Figure 3. Effect of initial concentration and treatment time for operating conditions of current density = 22 mA/cm^2; pH_0 = 7. 50; and treatment time = 30 min

Effect of current density

In all electrochemical processes, current density is the most important operating parameter for controlling the reaction rate inside the electrochemical reactor, as it determines the quantity and release rate of the coagulant into the treatment medium and the rate of bubble production. Hence, the current density controls the EC process performance and operating costs[40, 41]. Figure 4-a illustrates the impact of current density in the range of 13–40 mA/cm^2 on urea removal of 1.2 g/l initial concentration in synthetic wastewater. For all tested current densities, a significant increase in urea removal was observed during the first treatment period when the removal rate increases from 20.3% to 31.5% for a current density range of 13–31 mA/cm^2. This was followed by stabilization, then a minor decrease beyond the 9 minute mark. The growth in the yield of urea removed during the first 9 min of the treatment at high current applied to the anode can be ascribed to anode's dissolution, which

Table 1. Mathematical representations of the statistical indices

Tool	Abbreviation/ Symbol	Equation	Eq.No
Coefficient of determination	R^2	$1-\frac{\sum_{i-1}^{N}(y_i-y_i^*)^2}{\sum_{i=1}^{N}(y_i-\bar{y})^2}$	(11)
Mean squared Error	MSE	$\frac{1}{N}\sum_{i=1}^{N}(y_i-y_i^*)^2$	(12)
Root Mean Squared Error	RMSE	$\sqrt{\frac{1}{N}\sum_{i=1}^{N}(y_i-y_i^*)^2}$	(13)

generates zinc oxides, oxyhydroxides, and hydroxides, and the subsequent gas bubble formation. Each of those provide active surfaces for urea adsorption, resulting in a greater quantity of urea uptake and removal[42, 43]. The degree of urea removal is substantially impacted by the desorption phenomena that may occur in the concluding phase of the process[5, 7]. Finally, a passivation layer on the anode surface may also exist, which would negatively impact the rate of urea removal[4, 44] and possibly explain the moderate urea removal yields reported by other[7, 23]. Herein, urea removal rate with both 13 40 mA/cm^2 and 40 40 mA/cm^2 were found to be highly inefficient. While the 22 mA/cm^2 and 31 mA/cm^2 current settings achieved nearly equivalent removal levels at around 9 minutes, the 31 mA/cm^2 current density yielded better early performance. The results are influenced by the fact that high generation rates of hydrogen bubbles generate density and local turbulence that may impede the agglomeration of zinc hydroxide particles responsible for coagulation, thus hindering the elimination of dissolved urea[7].

Figure 4-b shows theoretical dissolved zinc concentration values – calculated after Faraday's law in the 0.5 L volume solution-anode weight loss after 30 min and faradaic yield at different current densities (13, 22, 31, and 40 mA/cm^2). The results show a positive correlation with current density: dissolved Zn^2 concentration varied from 183.01 to 549.04 mg/L, and anode weight loss from 178.4 mg to 599.61 mg. The faradaic yield of zinc dissolution was, thus, found to pass from 1.175 to 1.092, which shows the occurrence of zinc corrosion favored by the presence of chloride ions.

The cell voltage rise from 4.3 V to 11.8 V was principally caused by the prevailing contribution of ohmic drop energy consumption. This resulted in a variation in specific energy 1.29 to 10.44 kWh/m^3 after 30 min varied. Based on the results in Figure 4- a,b, a current density of 22 mA/cm^2 was chosen for subsequent tests, as it enabled maximum urea removal (30%) to be achieved in 9 minutes, at which time approximately 101 mg Zn was dissolved from the anode, and the specific energy was only at 1.14 kWh/m^3. In summary, at 22 mA/cm^2, a balance between minimal costs and waste was achieved with respect to maximum removal.

Fig. 4-c shows SEM image of the zinc anode prior to the EC process. The pristine anode surface was observed as uniform and homogenous except for small scratches, likely due to the mechanical handling of metal during the electrode shaping process. In contrast, the post-EC process SEM image (Fig. 4-d) is highly inhomogeneous, with the presence of dents and cavities caused by zinc dissolution upon chloride ions, known to induce pitting corrosion.

Effect of initial pH solution

The solution's initial pH (pH_i)level is known to strongly influence EC performance, because of its dissolution of the electrodes, the speciation of the hydrolysis products, and the mechanism of ions and pollutant removal[45]. Experimental tests were conducted at a current density

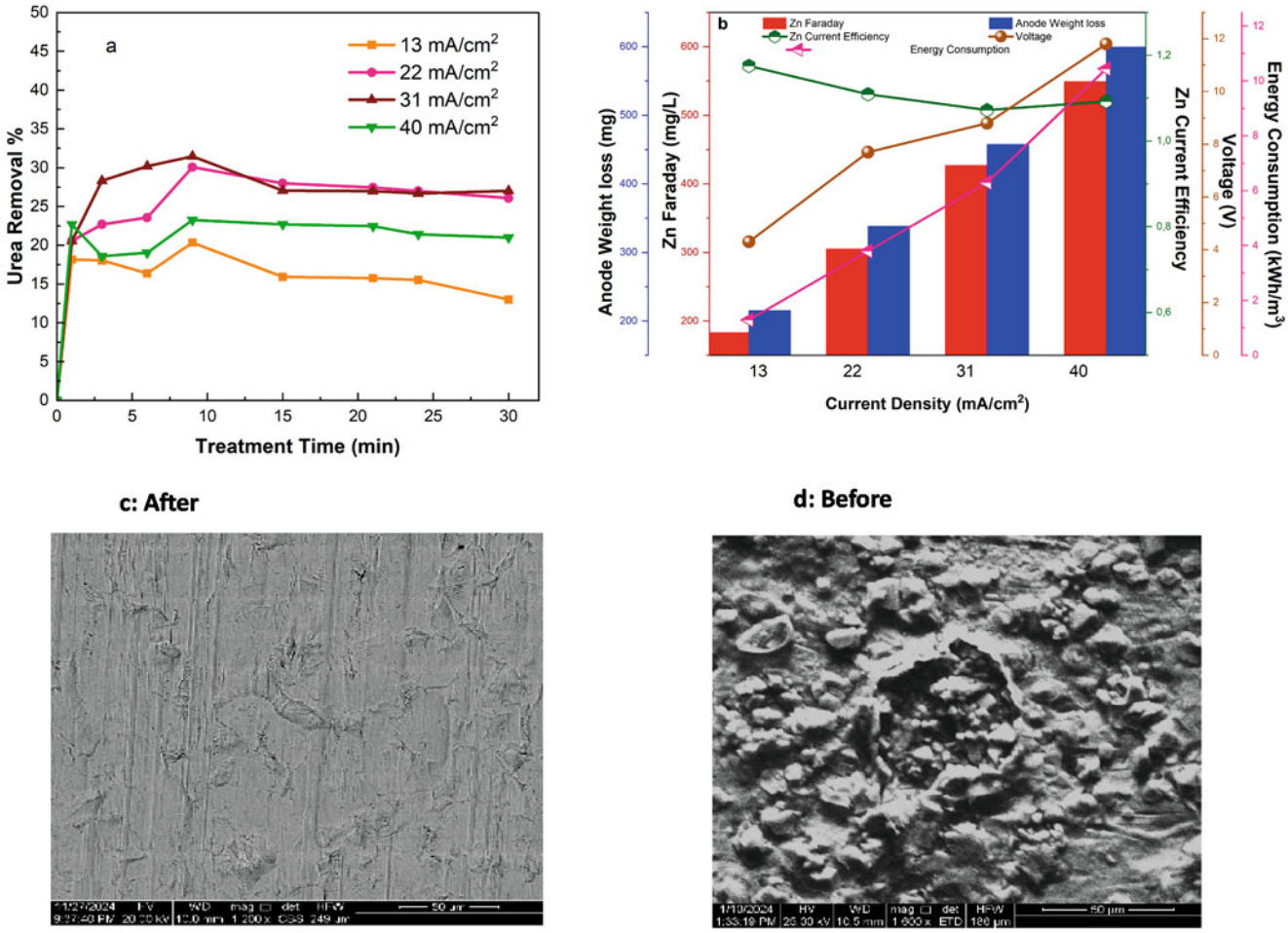

Figure 4. Effect of current density on: (a) removal of urea; (b) electrocoagulation variables; and (c-d) SEM of Zinc anode Operating conditions: $[Urea]_0$ = 1.2 g/L; pH_0 = 7.50; Treatment time: 30 min.

of 22 mA/cm² with pH_i values 4.09, 7.6, and 10.13. Figure 5a shows clearly superior performance (faster and more removal) with pH_i of 10.13. With that, removal reached 42 % after only 6 minutes of treatment. However, with 9 minutes, the solutions with pH_i of 4 achieved 27% and pH_i of 7 reached 30% This was expected as under alkaline conditions (pH > 8.6), other researchers, when removing nickel observed the formation of insoluble amorphous $Zn(OH)_2$, exhibiting large surface areas, which is beneficial for efficient adsorption of soluble organic compounds[46]. The moderate yields in the other pH zones can be explained by the fact that the pH usually increases during the EC treatment (see Fig. 5-a), where the fastest rate of pH change during EC units is when pH varied between 4 and 7 and reached 7 and 8 after 30 minutes of treatment, and this coincides with the start of the formation of $Zn(OH)_2$.

Urea removal rates herein exceeded those by Safwat et al; 2020[7], who reported 35% urea removal at pH 7. However, to avoid adding chemicals, keeping the "natural" pH of the solution at 7.60 for the following EC runs was preferred. Figure 5-b illustrates the mechanisms of urea elimination during EC at pH_i 7.60. The Zn^2_2 produced by electro-dissolution reacts with OH^- ions provided by water and electrodes to form various zinc monomers and polymer species, which finally transform into insoluble amorphous $Zn(OH)_2$ through complex polymerization[46], which acts as a coagulating agent. These solids aggregate urea particles into larger aggregates. Additionally, the precipitates formed can adsorb urea through electrostatic attraction, hydroxyl exchange, and surface complexation. Finally, during hydrogen bubble-induced flotation, the foam formed on the solution surface can also adsorb urea, thus eliminating it.

Effect of electrolyte concentration

In EC processes, electrolyte concentration is a crucial component as it affects first the solution's conductivity, thus the ohmic drop and the energy loss by Joule effects at a fixed current density[36]. Secondly, the initial electrolyte concentration impacts corrosion (especially when using chloride salts). Thus the divalent zinc formation rate at the anode impacts urea removal efficiency[37]. The results of experiments conducted with different NaCl concentrations in 1.2 g/L urea solution at a constant current density of 22 mA/cm² and a natural pH are presented in Figure 6. The concentration of NaCl negligibly affects the rate of the process. A slight improvement in urea removal yield was observed before 9 minutes of electrolysis. Also, around the processing time, yields tended to converge at about 30%. The enhancement in the elimination rate of urea by adding higher NaCl concentration is attributed by many authors[47] to the contribution of Cl^- anions to the dissolution of the metallic anode by pitting corrosion, which leads to a high amount of Zn^{2+} ions that increase the production of $Zn(OH)_2$ which causes higher elimination of urea. El Gheriany et al., 2022[3] explained that the introduction of more NaCl in the solution increases conductivity and induces a higher screening for the electrostatic interactions, which could improve pollutant capture by hydroxides[3]. Those authors also reported that an increase in water conductivity contributes to the reduction in the required voltage for achieving a certain current density due to the mitigation of the ohmic drop (IR) and, hence, decreasing the power requirement of EC[3].

Notably, the 30% yield diminished during the remaining time from 10 to 30min, and adding more NaCl did not significantly improve removal (Fig. 6). All reached maximum removal around 9 minutes with best result of 26% achieved with a 0.5 g/L NaCl concentration and the worst of 24% with a 1.0 g/L NaCl concentration. Similar results were obtained by Chen[48, 49] with other pollutants and in the presence of other metal salts[50]. These results may be attributable to the potential deposition of cations (Na^+, Cl^- and Zn(II)) and sludge particles on the surface of the electrode material. This would form an oxide layer, thereby inhibiting the dissolution of metal and, thus, reducing electrode dissolution with additional treatment time[51, 52] So, NaCl concentration of 1.5 g/L was chosen as the best due to the solution conductivity being deemed sufficient to give the highest rate of urea elimination with a minimum energy consumption.

Effect of the electrode gap

Inter-electrode distance (ID) plays a key role in energy consumption and pollutant removal effectiveness in the EC due to its influence on the ohmic resistance[53]. The influence was explored herein by changing the gap between electrodes from 1 to 2 to 3 cm, when the initial

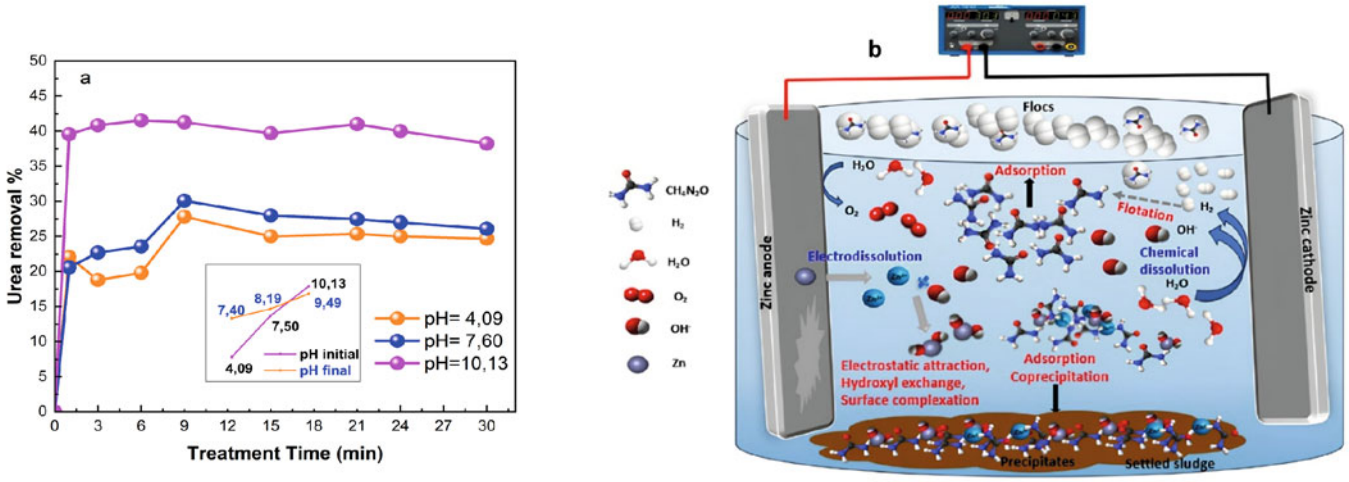

Figure 5. (a) Effect of initial solution pH on urea removal; (b) Proposed electrocoagulation mechanisms of urea. Operating conditions: [Urea]= 1.2 g/L; current density = 22 mA/cm²; Treatment time: 30 min.

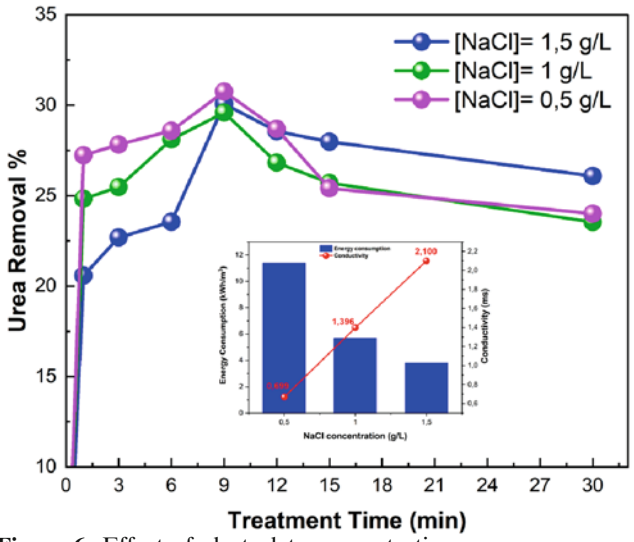

Figure 6. Effect of electrolyte concentration.
Operating conditions: [Urea] = 1.2 g/L; Current density = 22 mA/cm^2; Treatment time: 30 min; pH_0 = 7.60

urea concentration, current density, and initial pH were kept constant at 1.2 g/L, 22 mA/cm^2, and real pH, respectively. Figure 7 shows that urea removal is inversely proportional to the ID, with the best urea elimination (R = 30%) attained with the smallest gap at 1 cm. This dropped to 27% and then to 25% as the distance was increased to 2 cm and then to 3 cm. This was expected because with a large inter-electrode distance, the ionic interactions between pollutants and the hydroxide polymer and electrostatic attraction are limited, leading to a reduction in the pollutant removal yield[44, 54]. Similar results were reported by Medna Collona et al. (2024) and A. Kilani (2025), who optimized an inter-electrode distance of 1 cm[55, 56]. Figure 7 also shows the higher yield removal was accompanied by lower energy consumption. In balancing removal rate and the energy consumption, the electrode gap was kept at 1 cm in the following EC runs because of the rate of 30% which is very close to 3.8 kWh/m³, which corresponds to the highest efficiency while consuming more energy.

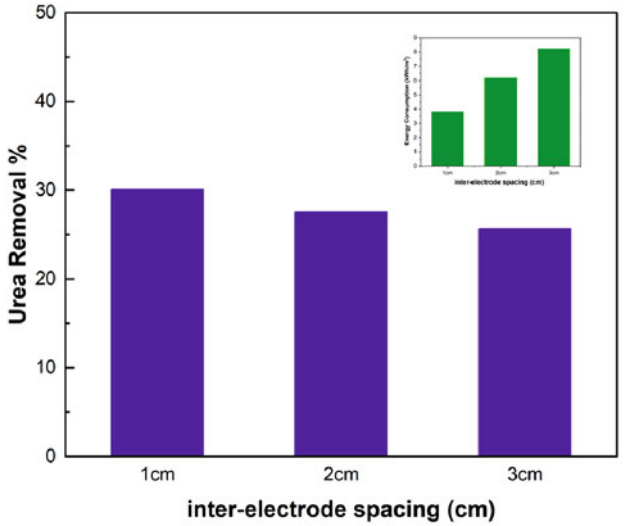

Figure 7. Effect inter- electrode spacing.
Operating conditions: [Urea]= 1.2 g/L; Current density = 22 mA/cm^2; Treatment time: 9 min; pH0 = 7.60

Effect of temperature

Temperature strongly impacts the nature and strength of adsorption during EC (Fig. 8). Higher temperatures increase ion mobility and collision rates[57, 58], as well as the activity of the adsorbent surface[59], and the dissolution rate of the electrodes, which relates to the formation rate of hydroxyl ions[60, 61]. This was tested at 10, 20, 30, and 40 °C, with natural pH, an ID of 1 cm, and a current density of 22 mA/cm^2 kept constant. After 15 min, the urea removal rate decreased from 40% to 22% as the temperature increased from 10 to 40 °C. This is attributable to the increasing water temperature adversely influences the solubility of the coagulant generated[62]. Moreover, increasing the collision rate between flocs might degrade them[63].

As also shown in Figure 8, energy consumption is inversely proportional to water temperature. Therefore, room temperature (20 °C) was considered the optimal condition, since the removal efficiency (30%) is close to that of 10 °C but with lower energy consumption.

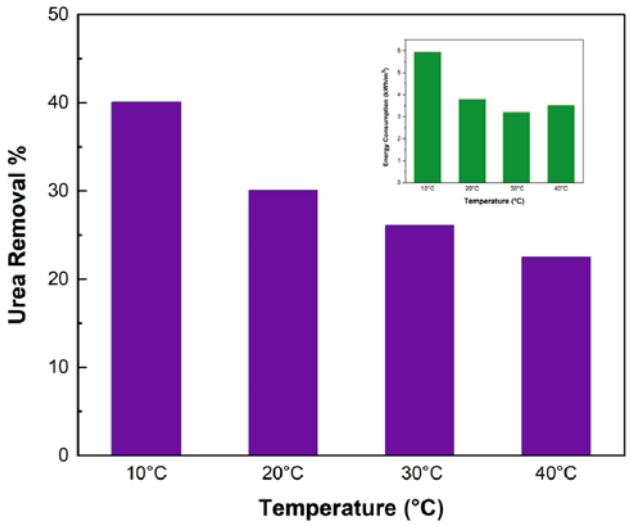

Figure 8. Effect of temperature.
Operating conditions: [Urea]= 1.2 g/L; Current density = 22 mA/cm^2; Treatment time: 9 min; pH0 = 7.60

Notably, solution temperature is enhanced by the Joule effect owing to the higher ohmic resistance of the EC cell, especially at lower concentrations of electrolyte and larger electrode gaps. Even though other phenomena are to govern the efficiency of EC processes, and although no quantitative correlation could be established, the three operating conditions – temperature, electrolyte concentration, and electrode gap – are inter-related.

Gradient Boosting Regressor Model Analysis

To further optimize parameters within the experimental space without undertaking further exploratory testing, a GBR model with various hyperparameters (number of estimators, learning rate, maximum depth) was implemented by varying the random state parameter to improve the target variable, namely the EC cell current in Amp. The results exhibited significant variability in R^2 scores, ranging from a perfect 1.0 with random state = 43 (with possible overfitting) to very low negative values such as -7.357 for random state = 45– suggesting underfitting, where model performance is worse than a simple mean of the data.

Optimization and Cross-Validation

In the model optimization procedure, cross-validation using GridSearchCV and KFold methodologies was employed to enhance the model's performance. This allowed for more optimal values for the procedure parameters to be identified. A learning rate of 0.5 s^{-1}, a maximum depth of 5 (5-fold cross validations), and n = 200 estimators were used. That achieved an RMSE of 0.0166, an MSE of 0.000276, and an R^2 of 0.9825 (Table 2), indicating excellent performance and robust generalization to new data.

Figure 9-a presents a regression plot based on the complete dataset (combining training and testing data). Each observation is represented by a point scattered around a red dashed line, which serves as a reference. The proximity of the points to this line indicates a strong correspondence between the model's predictions and the target values. A tightly clustered distribution around the red line reflects accurate predictions, while a more scattered distribution suggests prediction errors. In figure 9-a, the observed agreement between the predicted and target values highlights the good performance of the GBR model in capturing the underlying relationships within the data.

Figure 9-b presents the Cook's Distance plot for the regression model. The threshold value is equal to 4/n, i.e. 0.02 in the present case. The Cook's Distance spikes compared to this minimum value. Most values are below 0.02, with some clustering near zero, showing that most of the data points exert little influence on the model. The most prominent spike occurs at approximately observation 25, with a Cook's Distance value reaching about 0.11.

Figure 9-c is a scatter plot of "Residuals vs Leverage" showing most data points clustered in the lower left corner, indicating low leverage and low residuals for the majority of observations. Training Loss Curve on Figure 9-d illustrates how the training loss of GBR model changes over the course of boosting iterations. The curve starts at a relatively high loss value (around 0.004) at the beginning of training and drops very rapidly in the first few iterations, showing a steep decline. From about iteration 10 onwards, the loss remains very close to zero (below 10^{-5}, with minimal further decrease, indicating that the model learns quickly in the initial iterations, making significant improvements in reducing the training error. The overall features and performances of the model generated by the GBR method are summarized in Table 2.

Analysis of the GBR model for the Current Intensity (A) variable revealed insights into the model's performance. The residuals ranged from –0.161053 to 0.066762, with the majority clustered very close to zero. This suggests

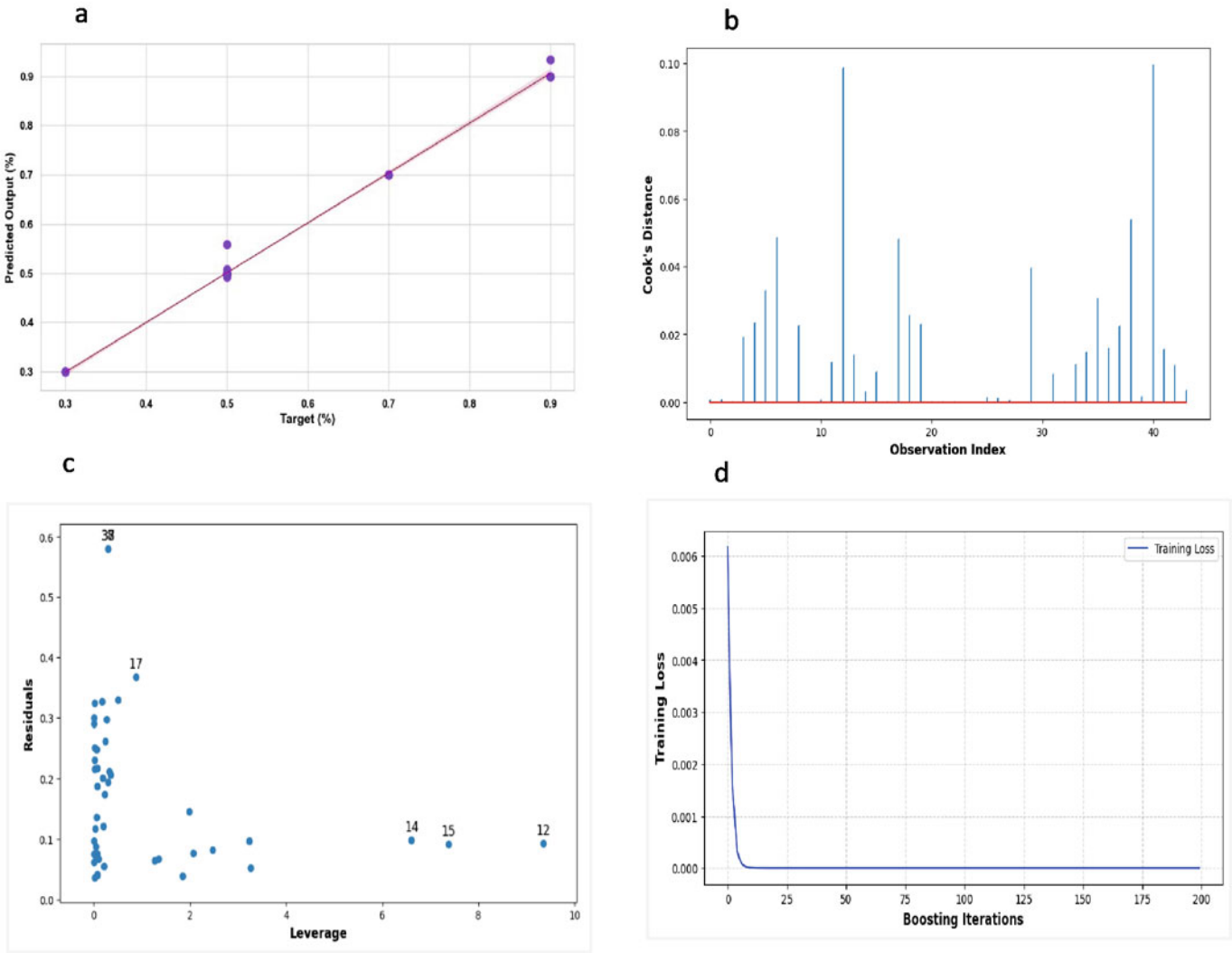

Figure 9. GBR Model Results: (a) Regression Plot for Full Dataset; (b) Cook's Distance Plot; (c) Residuals vs. Leverage Plot in the Selected Model; (d) Loss Curve

Table 2. Characteristics of the developed GBR model

Methods	
Characteristic	Value
Training Algorithm	Gradient Boosting Regressor (GBR)
Data Division	Train/Test Split
Percentage Data Sharing	85% Training, 15% Testing
Number of Estimators (Epochs)	200
Validation Checks	5-Fold Cross-Validation
Mathematical Model	Ensemble of Decision Trees
Results	
Best Model Parameters	
- Learning Rate	0.5
- Maximum Depth	5
- Number of Estimators	200
Evaluation Metrics	
- RMSE (Root Mean Squared Error)	0.01666
- MSE (Mean Squared Error)	0.0002897
- R^2 (Coefficient of Determination)	0.9825

that the model generally provides accurate predictions for most observations. Overall, these methods and analyses confirm that the GBR model is robust, exhibits performance metrics, and provides reliable predictions for the target variable.

Enhanced urea removal through electrocoagulation combination

Different treatment combinations were tested to assess the efficiency of urea removal. The first approach combined EC and chemical coagulation (CC) in two series of experiments: (1) EC followed by CC (EC-CC), then CC followed by EC (CC-EC), and (2) successive cycles of EC, where, after each cycle, the solution was filtered and the filtrate used for the next cycle until four consecutive cycles of EC were reached (EC-EC-EC-EC). All experiments were conducted under previously optimized conditions: urea concentration of 1.2 g/L, NaCl concentration of 1.5 g/L, pH of 7.60, and a treatment time of 9 minutes.

Firstly, jar test runs were conducted to determine the optimal coagulant dosage for urea removal. Different doses of zinc sulfate were applied during chemical coagulation, ranging from 2 to 8 g/L, corresponding to 0.68–2.72 g/L Zn(II). Figure 10-a shows that the urea removal rate increases with higher concentrations of coagulant to reach a maximum rate (21%) for a dose of 6 g/L. Although the amount of coagulant is higher compared to the theoretical amount of zinc generated by EC, its efficiency is significantly smaller than that obtained with EC. This observation, whereby the quantity of chemical coagulant used is higher than that generated by electrocoagulation, aligns with the findings of previous studies. This is probably due to the fact that zinc cations electrochemically generated can convert to zinc hydroxide coagulant upon steady evolution of hydroxide ions at the cathode, whereas in chemical coagulation, hydrolysis of zinc sulfate results in a decrease in pH, which can affect the efficiency of urea removal[7, 50]. This result is higher than that reported by A. Shaban et al. (2023)[4] including the proliferation of algae as a consequence of eutrophication as well as the discharge of ammonia, which exerts a detrimental impact on aquatic organisms. To assess the efficacy of several treatment strategies for lowering urea concentrations, this study compared the removing performances of electrocoagulation (EC, who observed that urea removal did not exceed 6% when using ferric metallic salts at an optimal dose of 0.5 g/L[4]. It also surpasses the findings of another study by the same author (A. Shaban et al., 2024[64]), which applied the same 0.5 g/L dose using various aluminum-based coagulants (sulfate, chloride, and alum)[64]. In contrast, Safwat & Matta (2020)[7] achieved a high urea removal efficiency by applying a high $ZnSO_4$ concentration of 160 g/L, although their treatment operating conditions differed from ours. In any case, to limit the potential hazard from the introduced zinc sulfate, its concentration was restricted to 2 g/L, in spite of the slightly lower efficiency at 17%. As shown in figure 10-b, the implementation of the CC-EC method achieved a higher removal efficiency in synthetic wastewater (35%) compared to EC-CC method when the urea removal rate is of 24%. This could be due to several factors. First, in the case of EC-CC, the zinc ions electrochemically generated during the EC could be more reactive or available for coagulation than the zinc ions formed by the dissolution of zinc sulfate during the CC. In addition, the EC could promote the formation of larger or more stable flocs that are easier to remove by filtration. On the other hand, in the case of CC-EC, the initial addition of zinc sulfate could interfere with the EC or alter the water conditions (for example, by decreasing the pH), which could affect the efficiency of the EC.

For the second approach, consisting of cycles of EC, Figure 10-c shows an increase in urea removal efficiency (R = 42%) compared to a single EC (R = 30%) and a stabilization of the efficiency after the second EC (EC-EC). The increase in efficiency can be attributed to the progressive accumulation of zinc ions in the solution, thereby increasing the active sites available for urea coagulation. The stabilization after the second EC suggests that the majority of zinc ions necessary for effective coagulation are already present after two cycles, and additional cycles do not bring significant improvement, indicating a saturation of the coagulation sites. This is consistent with the conclusions drawn for the single EC runs discussed in Section 3-1.

Cost Analysis (consumption of electricity, and electrodes)

Based on the optimized experimental results presented above, cost analyses were calculated for the different methods employed, whether electrocoagulation was used alone or in combinations, as shown in Table 3. The 4-cycle EC method shows the highest energy consump-

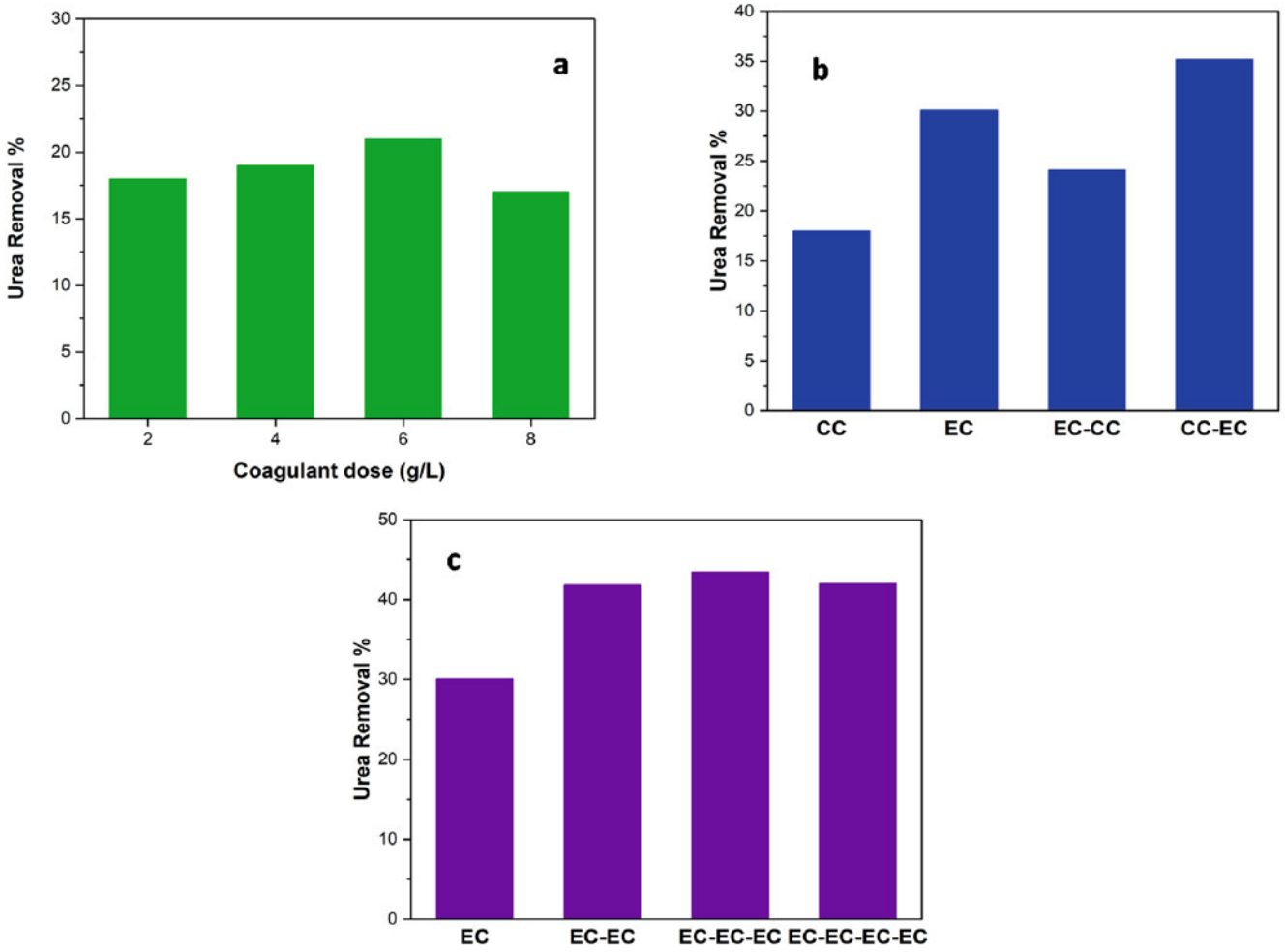

Figure 10. Urea removal efficiency by: (a) Chemical coagulation; (b) EC-CC and CC-EC combination; and (c) EC cycle

tion, reaching 3.96 kWh/m^3, while the single EC method shows the lowest consumption at 1.14 kWh/m^3. In terms of electrode consumption, an increase in the number of cycles led to a corresponding increase in electrode consumption. Cost estimation showed that the 4-cycle EC method is the most expensive, while the simple EC method is the least expensive.

For the EC-EC and EC-EC-EC method, the average cost was found near $ 4.876/m^3, assuming no recycling or reuse of the electrolyte. The large operation cost of mixed CC-EC combinations is principally caused by the cost of added zinc sulfate: the point is to define how such electrolyte, partly in the form of zinc hydroxide could be reused, for instance as fertilizers for agriculture. However, for the sake of simplicity, use of only electrocoagulation processes is recommended. The EC-EC combination offers the maximum urea removal rate of near 43% for a treatment cost around US$ 1.334 (about 27% of the EC-EC and EC-EC-EC approaches.

Table 4 presents a comparison between energy expenditure and electrode consumption for electrocoagulation treatment of urea, using various electrode materials under optimum conditions. The examples differ by electrode material, ID gap and the electrolyte concentration. Because of the predominance in ohmic drop in the cell voltage in most EC processes, the voltage and the energy demand vary nearly linearly with the electrode gap. Besides, the two first papers with various metals considered employed current densities that are somewhat near to those of this study, but this has resulted in more energy demands.

Comparing our results with those presented in the table, we find that the electrode expenditure and energy consumption are acceptable. However, it is important to

Table 3. Operating cost calculation for EC process

	Technique or combination considered			
Electrocoagulation	EC	EC-EC	EC-EC-EC	EC-EC-EC-EC
Energy consumption (kWh/m^3)	1,14	2,1	3,55	3,96
Electrode consumption (kg/m^3)	0,203	0,406	0,609	0,812
Cost calculated ($/m^3)	0,676	1,334	2,016	2,66
Electrocoagulation + chemical coagulation		EC-CC	CC-EC	
Energy consumption (kWh/m^3)		1,14	1,14	
Electrode consumption (kg/m^3)		0.203	0.203	
Zinc sulfate consumption (kg/m^3)		2	2	
Reactant cost ($/m^3)		4,83	4,83	
Cost calculated ($/m^3)		4,876	4,876	

Table 4. Energy and electrode consumption for electrocoagulation treatment of urea. In the table, "cd" is for current density. Removal rate of urea varied from 40% to 66%

Electrode type	Optimum Conditions	Energy consumption (kWh/m^3)	Electrode consumption (g/m^3)	Reference
Fe	U = 12 V, gap = 3 cm	112.8	9.8	5
Cu	[Urea]= 1 g/L [NaCl] = 0.4 g/L U = 6 V, 3 cm	32.4	6.4	
Zn	[$MgCl_2$] = 2 g/L cd = 21 mA/cm^2 gap = 2 cm	4.09	240	7
Zn	[Urea]= 1.2 g/L [NaCl] 1.5 g/L cd=22 mA/cm^2 gap=1 cm	1.14	203	This study

note that performance can vary depending on the specific pollutant and operating conditions. Electrocoagulation remains a promising method for wastewater treatment.

Application of optimum electrocoagulation conditions on real wastewater

The study focused on treating real hospital wastewater effluent (dialysate) from a hemodialysis service, characterized by 1.3 g/L of urea, a pH of 10, and a conductivity of 9.1 mS/cm. The EC conditions used in this study are those optimized in Section III.1 (a current density of 22 mA/cm^2 and a treatment time of 9 minutes). The obtained results (Fig. 11) show a urea elimination rate close to 27% after 9 minutes of treatment. The decrease in efficiency compared to synthetic effluents is attributed to various organic and inorganic compounds in the real effluent, which can interfere with the EC treatment process. Consequently, a portion of the coagulant formed was utilized to eliminate other pollutants, such as color, rather than urea. The treatment of real effluent from dialysate required an energy consumption of 1.75 kWh per cubic meter, resulting in a total cost of 0.0728 USD/m^3. These findings highlight the economic viability of this electrochemical approach for managing dialytic wastewater.

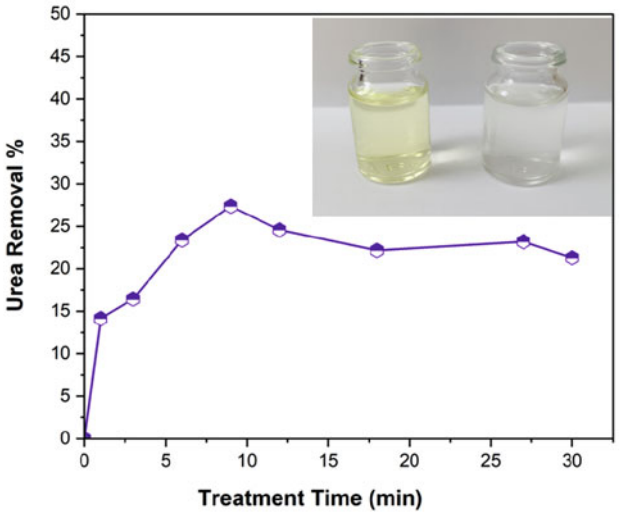

Figure 11. Removal of urea from real wastewater (dialysate)

Electrocoagulation sludge characterization

Characterization of the EC treatment sludge produced after EC treatment conditions is crucial to assess its potential reuse and valorization. With a urea concentration of 1.2 g/L, current density of 22 mA/cm^2, and a pH of 7.60, the sludge powder exhibits no oriented morphology but fine and coarse agglomerated particles in the form of irregularly sized aggregates, without well-defined crystals (Fig. 11-a). This surface SEM image is consistent with those presented by Kamrul and Nediljka[65, 66]. The absence of well-defined crystals and the presence of irregular-sized aggregates suggest that the EC process favors the formation of amorphous particles, probably due to the rapid formation of solid metal hydroxide in the EC process of electrochemical coagulation. EDS analysis of the electrocoagulated sludge confirms the adsorption of organic matter from urea. The major elements identified are oxygen (O), sodium (Na), and zinc (Zn), while nitrogen (N), carbon (C), and chlorine (Cl) are present in smaller quantities. The majority presence of oxygen, sodium, and zinc indicates that these elements play a key role in sludge formation, with oxygen coming from water or air, sodium from the NaCl used, and zinc from the electrodes. The adsorption of organic matter, such as urea, onto the sludge particles demonstrates the effectiveness of EC in removing organic pollutants from water, underlining this technique's potential for treating water containing organic compounds.

A detailed FTIR analysis of the electrocoagulated sample was conducted to examine its functional groups. Figure 11-b illustrates that the sludge sample shows several bands, which indicate the presence of urea compounds. The frequency range 2800–3400 cm^{-1} indicates the presence of the OH group, largely present in the water still contained in the sludge[5, 7]. Frequencies of 3300–3400 cm^{-1} correspond to N-H stretching, while the band at 1618 cm^{-1} is associated with urea C=O, and that at 1466 cm^{-1} with C-N stretching[4]. All of these peaks confirm the presence of urea on the sludge surface.

The crystalline composition of the sludge was analyzed using XRD. Figure 10-c shows that the predominant material in the crystallographic structure of the sludge is zinc. The intensity peaks at 31.7°, 34.40°, and 36.1° probably correspond to $Zn(OH)_2$[67]. In addition, the sharper peaks at 38° and 44.28° are probably due to ZnO. Consequently, considering the sharp and weak peaks, the compounds present are likely $Zn_5(OH)_8Cl_2$-H_2O derivatives[68].

Average, physico-chemical analysis of the sludge obtained during electrocoagulation shows that oxygen, zinc, Carbone and azote, and sodium are the main components and could be valorized in land-based applications or as a coagulant or as a sorbent for a multitude game of pollutant[69]. Metals could be recovered from wastewater treatment sludges, Rodriguez et al. (2020)[70], and Liu and Wang (2008)[71] demonstrated the effective recovery of zinc from wastewater sludge by both chemical or electrochemical techniques. In 2007, Hegazy[72] showed that wastewater sludge has potential for utilization as a construction material.

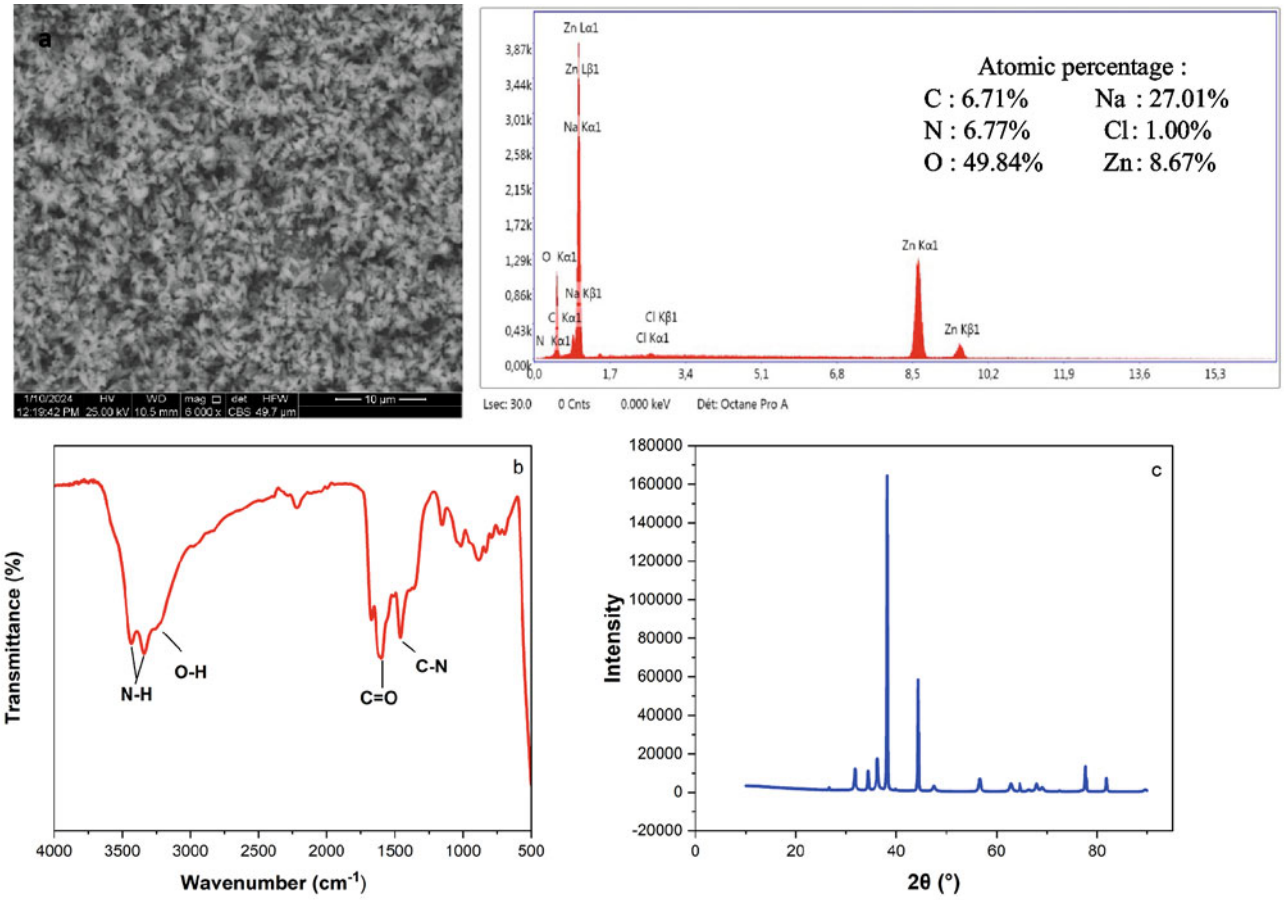

Figure 12. Sludge characterization: (a) SEM-EDS; (b) FTIR; and (c) XRD

CONCLUSIONS

The main objective of this study was to evaluate the effect of operating EC parameters applied to remove urea from synthetic and real wastewater effluents. By examining the obtained results, at an initial urea concentration of 1.2 g/L, a maximum removal efficiency of 42% was achieved throughout minutes with a current density of 22 mA/cm^2 and a pH solution of 10. Maintaining the natural pH of the solution (~7.60) provided a notable yield for both synthetic urea solution (30%) and real hospital effluent (27%), while eliminating the need for chemical additives.

Application of the GBR model leveraging Artificial Intelligence (AI) demonstrated a high predictive accuracy, enabling further parameter optimization with predictive performance of (R^2 = 0.9825; RMSE = 0.01666). Combined treatments EC–CC and CC–EC showed moderate improvement, reaching up to 35% efficiency when chemical coagulation preceded EC. However, successive EC cycles (EC–EC) proved to be the most effective and economically favorable strategy, achieving a 42% removal rate with a moderate treatment cost of $1.33/m^3.

Physicochemical analysis of the EC-generated sludge revealed an amorphous structure rich in zinc, sodium, nitrogen, and carbon—features conducive to valorization as a coagulant or adsorbent in further research. Finally, applying the process to real hospital effluent confirmed its industrial feasibility.

In conclusion, this research proposes a sustainable and optimized solution for urea treatment in wastewater, while opening promising avenues for the reuse of solid by-products generated through the process.

LITERATURE CITED

1. Urbańczyk, E., Sowa, M. & Simka, W. (2016). Urea removal from aqueous solutions—a review. *J. Appl. Electrochem*. 46(10),1011–1029. DOI: 10.1007/s10800-016-0993-6.

2. Weerakoon, D., Bansal, B. & Padhye, L.P. (2023). A critical review on current urea removal technologies from water: An approach for pollution prevention and resource recovery. *Sep. Purif. Technol*. 314 (February), 123652. DOI:10.1016/j.seppur.2023.123652.

3. El Gheriany, I., Abdel-Aziz, M.H., El-Ashtoukhy, E.S.Z. & Sedahmed, G.H. (2022) Electrochemical removal of urea from wastewater by anodic oxidation using a new cell design: An experimental and modeling study. *Process Saf. Environ Prot*. 159,133–145. DOI: 10.1016/j.psep.2021.12.055.

4. Shaban, A., Basiouny, M.E. & AboSiada, O.A.(2023). Evaluation of Using Sequential Electrocoagulation and Chemical Coagulation for Urea Removal from Synthetic and Domestic Wastewater. *Water, Air, Soil Pollut*. 234(11).1–14. DOI: 10.1007/s11270-023-06743-5.

5. Mamdouh, M., Safwat, S.M., Abd-Elhalim, H. & Rozaik,. E. (2021). Urea removal using electrocoagulation process with copper and iron electrodes. *Desalin Water Treat*. 213, 259–268. DOI: 10.5004/dwt.2021.26690.

6. Chen, Y., Chen, H., Chen, Z., Hu, H., Deng, C. & Wang, X.(2021). The benefits of autotrophic nitrogen removal from high concentration of urea wastewater through a process of urea hydrolysis and partial nitritation in sequencing batch reactor. *J. Environ. Manage*. 292(May),112762. DOI:10.1016/j.jenvman.2021.112762.

7. Safwat, S.M. & Matta, M.E.(2020). Performance evaluation of electrocoagulation process using zinc electrodes for removal of urea. *Sep. Sci. Technol*. 55(14), 2500–2509. DOI: 10.1080/01496395.2019.1636067.

8. Kameda, T., Horikoshi, K., Kumagai, S., Saito, Y. & Yoshioka, T. (2020). Adsorption of urea, creatinine, and uric acid onto spherical activated carbon. *Sep. Purif. Technol*. 237,116367. DOI: 10.1016/j.seppur.2019.116367.

9. Mahalik, K., Sahu, J.N., Patwardhan, A.V. & Meikap, B.C. (2010). Kinetic studies on hydrolysis of urea in a semi-batch reactor at atmospheric pressure for safe use of ammonia in a power plant for flue gas conditioning. *J. Hazard Mater*. 175(1–3), 629–637. DOI: 10.1016/j.jhazmat.2009.10.053.

10. Shen, S., Li, M., Li, B. & Zhao, Z. (2014).Catalytic hydrolysis of urea from wastewater using different aluminas by a fixed bed reactor. *Environ. Sci. Pollut. Res*. 21(21), 12563–12568. DOI: 10.1007/s11356-014-3189-9.

11. Tan, T., Liu, S., Chen, K., Imhanria, S., Tao, P. & Wang, W. (2020). A multi-component system for urea electrooxidation: Ir3Sn nanoparticles loading on Iron- and Nitrogen- codoped composite carbon support. *J. Taiwan Inst. Chem. Eng*. 112, 116–121. DOI: 10.1016/j.jtice.2020.06.017.

12. Von Ahnen, M., Pedersen, L.F., Pedersen, P.B. & Dalsgaard, J. (2015). Degradation of urea, ammonia and nitrite in moving bed biofilters operated at different feed loadings. *Aquac Eng*. 69, 50–59. DOI:10.1016/j.aquaeng.2015.10.004.

13. Lu, J., Zhang, P. & Li, J.(2024). Mo(VI) removal from water by aluminum electrocoagulation: Cost-effectiveness analysis, main influencing factors, and proposed mechanisms. *J. Hazard Mater*. 461 (June 2023), 132608. DOI: 10.1016/j.jhazmat.2023.132608.

14. Pinedo-Hernández, J., Marrugo-Negrete, J., Pérez-Espitia, M., Durango-Hernández, J., Enamorado-Montes, G. & Navarro-Frómeta, A.(2024). A pilot-scale electrocoagulation-treatment wetland system for the treatment of landfill leachate. *J. Environ Manage*. 351(December 2023). DOI: 10.1016/j.jenvman.2023.119681.

15. Rangseesuriyachai, T., Pinpatthanapong, K., Boonnorat, J., Jitpinit, S., Pinpatthanapong, T. & Mueansichai, T. (2024). Optimization of COD and TDS removal from high-strength hospital wastewater by electrocoagulation using aluminium and iron electrodes: Insights from central composite design. *J. Environ. Chem. Eng*. 12(1),111627. DOI: 10.1016/j.jece.2023.111627.

16. Sivaranjani., G.A. & Ali, N. (2020). Applicability and new trends of different electrode materials and its combinations in electro coagulation process: A brief review. *Mater. Today Proc*. 37 (Part 2), 377–382. DOI: 10.1016/j.matpr.2020.05.379.

17. Cherifi, M., Belkacem, M., Hazourli, S., Debra, F.L. & Atba, W. (2023). A comparative study of hydrogen peroxide oxidation and electrocoagulation using aluminum, iron, and zinc electrodes for urban sludge disintegration. *Sep. Sci. Technol*. 58(10),1806–1820. DOI: 10.1080/01496395.2023.2213395.

18. Hashim, K.S., Shaw, A., Al Khaddar, R., Pedrola, M.O. & Phipps, D. (2017). Iron removal, energy consumption and operating cost of electrocoagulation of drinking water using a new flow column reactor. *J. Environ. Manage*. 189, 98–108. DOI: 10.1016/J.JENVMAN.2016.12.035.

19. Ali, I., Asim, M. & Khan, TA. (2013). Arsenite removal from water by electro-coagulation on zinc-zinc and copper-copper electrodes. *Int. J. Environ. Sci. Technol*. 10(2), 377–384. DOI: 10.1007/s13762-012-0113-z.

20. Fajardo, A.S., Rodrigues, R.F., Martins, R.C., Castro, L.M. & Quinta-Ferreira, R.M.(2015). Phenolic wastewaters treatment by electrocoagulation process using Zn anode. *Chem. Eng J*. 275, 331–341. DOI:10.1016/J.CEJ.2015.03.116.

21. Gong, C., Zhang, J., Ren, X., He, C., Han, J. & Zhang, Z. (2022). A comparative study of electrocoagulation treatment with iron, aluminum and zinc electrodes for selenium removal from flour production wastewater. *Chemosphere*. 303(P3), 135249. DOI:10.1016/j.chemosphere.2022.135249.

22. Hussin, F., Abnisa, F., Issabayeva, G. & Aroua, MK.(2017). Removal of lead by solar-photovoltaic electrocoagulation using novel perforated zinc electrode. *J. Clean Prod*. 147, 206–216. DOI: 10.1016/j.jclepro.2017.01.096.

23. Safwat, S.M., Mamdouh, M., Rozaik, E. & Abd-Elhalim, H. (2020). Performance evaluation of electrocoagulation process using aluminum and titanium electrodes for removal of urea. *Desalin Water Treat*. 191, 239–249. DOI: 10.5004/dwt.2020.25616.

24. Obi, C.C., Nwabanne, J.T., Igwegbe, C.A., Ohale, P.E. & Okpala, COR. (2022). Multi-characteristic optimization and modeling analysis of electrocoagulation treatment of abattoir wastewater using iron electrode pairs. *J. Water Process Eng*. 49 (June),103136. DOI: 10.1016/j.jwpe.2022.103136.

25. Gholami Shirkoohi, M., Tyagi, R.D., Vanrolleghem, P.A. & Drogui, P. (2022). A comparison of artificial intelligence models for predicting phosphate removal efficiency from wastewater using the electrocoagulation process. *Digit Chem. Eng*. 4(June), 100043. DOI: 10.1016/j.dche.2022.100043.

26. Onu, C.E., Nweke, C.N. & Nwabanne, J.T. (2022). Modeling of thermo-chemical pretreatment of yam peel substrate for biogas energy production: RSM, ANN, and ANFIS comparative approach. *Appl. Surf. Sci. Adv*. 11(April), 100299. DOI: 10.1016/j.apsadv.2022.100299.

27. Igwegbe, C.A., Obi, C.C. & Ohale, P.E. (2023). Modelling and optimisation of electrocoagulation/flocculation recovery of effluent from land-based aquaculture by artificial intelligence (AI) approaches. *Environ Sci. Pollut. Res*. 30(27), 70897–70917. DOI: 10.1007/s11356-023-27387-2.

28. Wang, G., Jia, Q.S., Zhou, M.C., Bi, J., Qiao, J. & Abusorrah, A. (2022). Artificial neural networks for water quality soft-sensing in wastewater treatment: a review. *Artif. Intell. Rev*. 55(1), 565–587. DOI: 10.1007/s10462-021-10038-8.

29. Touzani, S., Granderson, J. & Fernandes, S. (2018). Gradient boosting machine for modeling the energy consumption of commercial buildings. *Energy Build*. 158, 1533–1543. DOI: 10.1016/j.enbuild.2017.11.039.

30. Boulmaiz, A., Berredjem, H., Cheikchouk, K., Boulkrah, A., Aouras, H. & Djedi, H. (2024). Predicting HER2 Status Associated with Breast Cancer Aggressiveness Using Four Machine Learning Models. *Asian Pacific J. Cancer Prev*. 25(10), 3609–3618. DOI: 10.31557/APJCP.2024.25.10.3609.

31. Obi, C.C., Nwabanne, J.T., Igwegbe, C.A., Abonyi, M.N., Umembamalu, C.J. & Kamuche, T.T.G. (2024). Intelligent algorithms-aided modeling and optimization of the deturbidization of abattoir wastewater by electrocoagulation using aluminium electrodes. *J. Environ. Manage*. 353 (November 2023),120161. DOI: 10.1016/j.jenvman.2024.120161.

32. Otchere, D.A., Ganat, T.O.A., Ojero, J.O., Tackie-Otoo, B.N. & Taki, M.Y. (2022). Application of gradient boosting regression model for the evaluation of feature selection techniques in improving reservoir characterisation predictions. *J. Pet. Sci. Eng*. 208(May),109244. DOI: 10.1016/j.petrol.2021.109244.

33. Wang, H. & Gu, G. (2015). Wavelet gradient boosting regression method study in short-term load forecasting. *Smart Grid*. 5(4), 189–196. DOI: 10.12677/sg.2015.54023.

34. Fox, J. & Weisberg, S. (2018). *An R Companion to Applied Regression*. Sage publications.

35. Chan, K.M.A., Boyd, D.R. & Gould, R.K.(2020). Levers and leverage points for pathways to sustainability. *People Nat*. 2(3), 693–717. DOI: 10.1002/pan3.10124.

36. Bajpai, M., Katoch, S.S., Kadier, A. & Singh, A. (2022). A review on electrocoagulation process for the removal of emerging contaminants: theory, fundamentals, and applications. *Environ. Sci. Pollut. Res*. 29(11), 15252–15281. DOI: 10.1007/s11356-021-18348-8.

37. Asaithambi, P. (2016). Studies on various operating parameters for the removal of COD from pulp and paper industry using electrocoagulation process. *Desalin Water Treat*. 57(25), 11746–11755. DOI: 10.1080/19443994.2015.1046149.

38. Jing, G., Ren, S., Pooley, S., Sun, W., Kowalczuk, P.B. & Gao, Z. (2021). Electrocoagulation for industrial wastewater treatment: an updated review. *Environ. Sci. Water Res. Technol*. 7(7), 1177–1196. DOI: 10.1039/D1EW00158B.

39. El-Shazly, A.H. & Daous, M.A. (2013). Kinetics and performance of phosphate removal from hot industrial effluents using a continuous flow electrocoagulation reactor. *Int. J. Electrochem. Sci*. 8(1),184–194. DOI: 10.1016/s1452-3981(23)14012-0.

40. Khanaum, M.M. & Borhan, M.S. (2023). Electrocoagulation: An Overview of the Technology for Livestock Farm Wastewater Treatment. *Waste Technol*. 11(1), 1–16. DOI: 10.14710/wastech.11.1.1-16.

41. Bener, S., Bulca, Ö., Palas, B., Tekin, G., Atalay, S. & Ersöz, G. (2019). Electrocoagulation process for the treatment of real textile wastewater: Effect of operative conditions on the organic carbon removal and kinetic study. *Process Saf. Environ. Prot*. 129, 47–54. DOI: 10.1016/j.psep.2019.06.010.

42. Simka, W., Piotrowski, J. & Nawrat, G.(2007). Influence of anode material on electrochemical decomposition of urea. *Electrochim Acta*. 52(18), 5696–5703. DOI:10.1016/j.electacta.2006.12.017.

43. Simka, W., Piotrowski, J., Robak, A. & Nawrat, G. (2009). Electrochemical treatment of aqueous solutions containing urea. *J. Appl. Electrochem*. 39(7), 1137–1143. DOI: 10.1007/s10800-008-9771-4.

44. Hakizimana, J.N., Gourich, B. & Chafi, M. (2017). Electrocoagulation process in water treatment: A review of electrocoagulation modeling approaches. *Desalination*. 404, 1–21. DOI: 10.1016/j.desal.2016.10.011.

45. Atba, W., Cherifi, M., Grid, A., Debra, F.L. & Hazourli, S. (2023). Effect of Electrocoagulation Parameters on Chromium Removal, Sludge Settling, and Energy Consumption. *Anal. Bioanal. Electrochem*. 15(3), 166–183. DOI: 10.22034/abec.2023.703899.

46. Shaker, O.A., Safwat, S.M. & Matta, M.E. (2023). Nickel removal from wastewater using electrocoagulation process with zinc electrodes under various operating conditions: performance investigation, mechanism exploration, and cost analysis. *Environ. Sci. Pollut. Res*. 30(10), 26650–26662. DOI: 10.1007/s11356-022-24101-6.

47. Arroyo, M.G., Pérez-Herranz, V., Montañés, M.T., García-Antón, J. & Guiñón, J.L. (2009). Effect of pH and chloride concentration on the removal of hexavalent chromium in a batch electrocoagulation reactor. *J. Hazard. Mater*. 169(1-3), 1127–1133. DOI: 10.1016/j.jhazmat.2009.04.089.

48. Chen, G., Chen, X. & Yue, PL. (2000). E Lectrocoagulation and E Lectroflotation. *J Environ Eng*. 126(September), 858–863.

49. Uhlig, H.H. & Revie, R.W. (2000). *Uhlig's Corrosion Handbook*.

50. Comninellis, C. & Chen, G. (2010). *Electrochemistry for the Environment*. 2015.

51. Graça, N.S., Ribeiro, A.M. & Rodrigues, A.E. (2019). Modeling the electrocoagulation process for the treatment of contaminated water. *Chem. Eng. Sci*. 197, 379–385. DOI: 10.1016/j.ces.2018.12.038.

52. Tiaiba, M., Merzouk, B., Amour, A., Mazour, M., Leclerc, J.P. & Lapicque, F. (2017). Influence of electrodes connection mode and type of current in electrocoagulation process on the removal of a textile dye. *Desalin Water Treat*. 73, 330–338. DOI: 10.5004/DWT.2017.20502.

53. Safwat, S.M. (2020). Treatment of real printing wastewater using electrocoagulation process with titanium and zinc electrodes. *J. Water Process Eng*. 34(January), 101137. DOI: 10.1016/j.jwpe.2020.101137.

54. Safwat, S.M., Hamed, A. & Rozaik, E. (2019). Electrocoagulation/electroflotation of real printing wastewater using copper electrodes: A comparative study with aluminum electrodes. *Sep. Sci. Technol*. 54(1),183–194. DOI: 10.1080/01496395.2018.1494744.

55. Medina Collana, J.T., Ayllon Ormeño, M. & Julca Meza, C. Processes Coupled to Electrocoagulation for the Treatment of Distillery Wastewaters. *Sustain*. 16(15). DOI: 10.3390/su16156383.

56. Al-Kilani, M.R. & Bani-Melhem, K. (2025). The performance of electrocoagulation process for decolorization and COD removal of highly colored real grey water under variable operating conditions. *Desalin Water Treat*. 321 (November 2024), 100924. DOI: 10.1016/j.dwt.2024.100924.

57. Al-Raad, A.A. & Hanafiah, M.M. (2021). Removal of inorganic pollutants using electrocoagulation technology: A review of emerging applications and mechanisms. *J. Environ Manage*. 300 (February), 113696. DOI: 10.1016/j.jenvman.2021.113696.

58. Attour, A., Touati, M., Tlili, M., Ben Amor, M., Lapicque, F. & Leclerc, JP.(2014). Influence of operating parameters on phosphate removal from water by electrocoagulation using aluminum electrodes. *Sep. Purif. Technol*. 123, 124–129. DOI: 10.1016/j.seppur.2013.12.030.

59. Vasudevan, S., Lakshmi, J. & Sozhan, G. (2012). Toxicological & Environmental Chemistry Simultaneous removal of Co , Cu , and Cr from water by electrocoagulation. *Toxicol Environ. Chem*. 94 (December 2012), 37–41.

60. Vepsäläinen, M., Ghiasvand, M. & Selin, J. (2009). Investigations of the effects of temperature and initial sample pH on natural organic matter (NOM) removal with electrocoagulation using response surface method (RSM). *Sep. Purif. Technol*. 69(3), 255–261. DOI: 10.1016/j.seppur.2009.08.001.

61. Song, S., He, Z., Qiu, J., Xu, L. & Chen, J. (2007). Ozone assisted electrocoagulation for decolorization of C.I. Reactive Black 5 in aqueous solution: An investigation of the effect of operational parameters. *Sep. Purif. Technol*. 55(2), 238–245. DOI: 10.1016/j.seppur.2006.12.013.

62. El-Naas, M.H., Al-Zuhair, S., Al-Lobaney, A. & Makhlouf, S. (2009). Assessment of electrocoagulation for the treatment of petroleum refinery wastewater. *J. Environ. Manage*. 91(1), 180–185. DOI: 10.1016/j.jenvman.2009.08.003.

63. Khandegar, V. & Saroha, A.K. (2013). Electrocoagulation for the treatment of textile industry effluent - A review. *J. Environ. Manage*. 128, 949–963. DOI: 10.1016/j.jenvman.2013.06.043.

64. Shaban, A., Basiouny, M.E. & AboSiada, O.A. (2024). Comparative study of the removal of urea by electrocoagulation and electrocoagulation combined with chemical coagulation in aqueous effluents. *Sci. Rep*. 14(1), 1–14. DOI: 10.1038/s41598-024-81422-x.

65. Hassan, K., Farzana, R. & Sahajwalla, V. (2019). In-situ fabrication of ZnO thin film electrode using spent Zn–C battery and its electrochemical performance for supercapacitance. *SN Appl. Sci*. 1(4),1–13. DOI: 10.1007/s42452-019-0302-1.

66. Medvidović, N.V., Vrsalović, L., Svilović, S., Bilušić, A. & Jozić, D. (2023). Electrocoagulation treatment of compost leachate using aluminium alloy, carbon steel and zinc anode. *Appl. Surf. Sci. Adv*. 15 (December 2022). DOI: 10.1016/j.apsadv.2023.100404.

67. Kuchar, D., Fukuta, T., Onyango, M.S. & Matsuda, H. (2006). Sulfidation of zinc plating sludge with Na2S for zinc resource recovery. *J. Hazard. Mater*. 137(1), 185–191. DOI: 10.1016/j.jhazmat.2006.01.052.

68. Xu, Z., Ma, X., Liao, J., Osman, S.M., Wu, S. & Luque, R. (2022). Effects on the Physicochemical Properties of Hydrochar Originating from Deep Eutectic Solvent (Urea and $ZnCl_2$)-Assisted Hydrothermal Carbonization of Sewage Sludge. *ACS Sustain. Chem. Eng*. 10(13), 4258–4268. DOI: 10.1021/acssuschemeng.2c00086.

69. Nguyen, M.D., Thomas, M., Surapaneni, A., Moon, E.M. & Milne, N.A. (2022). Beneficial reuse of water treatment sludge in the context of circular economy. *Environ. Technol. Innov*. 28, 102651. DOI: 10.1016/j.eti.2022.102651.

70. Rodriguez, N., Gijsemans, L. & Bussé, J. (2020). Selective Removal of Zinc from BOF Sludge by Leaching with Mixtures of Ammonia and Ammonium Carbonate. *J. Sustain Metall*. 6(4), 680–690. DOI: 10.1007/s40831-020-00305-3.

71. Liu, S.H. & Wang, H.P. (2008). Fate of zinc in an electroplating sludge during electrokinetic treatments. *Chemosphere*. 72(11), 1734–1738. DOI: 10.1016/j.chemosphere.2008.04.077.

72. Hegazy, B.E. (2007). Brick making from water treatment plant sludge. *J. Eng. Appl. Sci*. 54(6), 599–615.